The 21 cm Signature of Cosmic String Wakes

Robert H. Brandenberger[1], Rebecca J. Danos[1], Oscar F. Hernández[2,1] and Gilbert P. Holder[1]

1) Department of Physics, McGill University, Montréal, QC, H3A 2T8, Canada
2) Marianopolis College, 4873 Westmount Ave., Westmount, QC H3Y 1X9, Canada
(Dated: October 13, 2018)

We discuss the signature of a cosmic string wake in 21cm redshift surveys. Since 21cm surveys probe higher redshifts than optical large-scale structure surveys, the signatures of cosmic strings are more manifest in 21cm maps than they are in optical galaxy surveys. We find that, provided the tension of the cosmic string exceeds a critical value (which depends on both the redshift when the string wake is created and the redshift of observation), a cosmic string wake will generate an emission signal with a brightness temperature which approaches a limiting value which at a redshift of $z + 1 = 30$ is close to 400 mK in the limit of large string tension. The signal will have a specific signature in position space: the excess 21cm radiation will be confined to a wedge-shaped region whose tip corresponds to the position of the string, whose planar dimensions are set by the planar dimensions of the string wake, and whose thickness (in redshift direction) depends on the string tension. For wakes created at $z_i + 1 = 10^3$, then at a redshift of $z + 1 = 30$ the critical value of the string tension μ is $G\mu = 6 \times 10^{-7}$, and it decreases linearly with redshift (for wakes created at the time of equal matter and radiation, the critical value is a factor of two lower at the same redshift). For smaller tensions, cosmic strings lead to an observable absorption signal with the same wedge geometry.

I. INTRODUCTION

Cosmic strings (see [1–6] for initial work on cosmic strings and structure formation) cannot be [7, 8] the dominant source of the primordial fluctuations, however they can still provide a secondary source of fluctuations. Over the past decade, the realization has grown that many inflationary scenarios constructed in the context of supergravity models lead to the formation of gauge theory cosmic strings at the end of the inflationary phase [9]. Also, in a large class of brane inflation models the formation of cosmic superstrings [10] at the end of inflation is generic [11], and in some cases (see [12]) these strings are stable (see also [13] for reviews on fundamental cosmic strings). Cosmic superstrings are also a possible remnant of an early Hagedorn phase of string gas cosmology [14]. In all of these contexts, both a scale-invariant spectrum of adiabatic coherent perturbations and a sub-dominant contribution of cosmic strings is predicted. Hence, it is important to search for the existence of cosmic strings.

In this paper we study the signature of cosmic strings in 21cm radiation maps (see e.g. [15] for an in-depth review of 21cm cosmology). Observing the intensity of the cosmological background radiation at wavelengths corresponding to the red-shifted 21cm transition line of neutral hydrogen has several potential advantages compared to the currently explored windows . First of all, it probes the distribution of the dominant form of baryonic matter and is thus not sensitive to our incomplete understanding of star formation and non-linear evolution, which is a problem when interpreting the results of optical redshift surveys. Secondly, it probes the universe at higher redshifts and allows us to explore the "dark ages" (the epoch before star formation and non-linear clustering set in). Related to this, it explores the distribution of matter in a regime when the amplitude of the fluctuations is smaller and linear theory is a better approximation. Finally, 21cm surveys provide three-dimensional maps, a significant potential advantage over CMB anisotropy maps.

Cosmic strings are known to give rise to distinctive signatures in CMB temperature anisotropy maps [16], CMB polarization maps [17] and large-scale structure (LSS) maps [18–23]. These distinctive signatures come from moving long (compared to the Hubble radius) strings (see Section 2). In the CMB temperature maps, these strings lead to line discontinuities, in the polarization maps to (roughly) rectangular regions with extra polarization, and in LSS maps to thin planar regions of enhanced density. These signals are manifest in position space maps, but they become obscured when calculating power spectra. Hence, the lesson is to study the maps in position versus momentum space.

Here, we compute the signature of a single cosmic string wake in 21cm emission. We find that strings with tensions μ somewhat below the current limits of $G\mu = 3 \times 10^{-7}$ could be detected in 21cm maps where they would appear as wedges in 21cm maps with either extra emission or extra absorption, depending on the tension and on the specific redshift. The planar dimensions are set by the direction of the string and its velocity vector, and the width of the wedges is proportional to the string tension. This signal must be searched for in position space maps. In Fourier space the distinctive phase information would be washed out.

The outline of this paper is as follows: In Section 2 we discuss how string wakes are generated and how these lead to distinctive signals for observations. We review gravitational accretion of matter onto cosmic string

wakes and compute the temperature of the HI gas inside the wake. In Section 3 we then study the 21cm emission signal from a single cosmic string wake. The generalization to the case of a network of string wakes will be addressed in a future publication. We compute the brightness temperature and describe the geometrical structure of the signal, a structure very characteristic for cosmic strings. In the final section we summarize our results and put them in the context of other work on the possible detection of cosmic strings. When computing the magnitude of the 21cm signal, we use the same WMAP concordance values [24] for the cosmological parameters as used in the review [15].

II. COSMIC STRINGS AND LARGE-SCALE STRUCTURE

In many field theory models, the formation of a network of cosmic strings is an inevitable consequence of a phase transition in the early universe (for reviews on cosmic strings see e.g. [25–28]). This network of cosmic strings approaches a "scaling solution" which means that the statistical properties of the string network are the same at all times if distances are scaled to the Hubble radius [28] . The detailed form of the scaling solution must be obtained from numerical simulations [29] of the evolution of a network of cosmic strings (see also [30] for some recent analytical work). There are two components of the string network - firstly a network of "long" strings with a mean curvature radius $\zeta = c_1 t$, where c_1 is a constant of order unity, and secondly a distribution of string loops with radii smaller than the horizon which results from the "cutting up" of the long string network as a consequence of string intersections. According to more recent cosmic string evolution simulations, the long string component is more important for cosmological structure formation.

Numerical simulations by different groups have clearly verified the scaling solution for the long string network. There is, however, still a large uncertainty concerning the distribution of string loops (the only agreement seems to be that the loops are less important than the long strings for cosmological structure formation). Hence, in order to obtain constraints in models with cosmic strings which are robust against the uncertainties in the numerical simulations, it is important to focus on signatures of long strings as opposed to signatures of string loops. The tightest current constraints on cosmic strings come from the shape of the angular power spectrum of CMB anisotropies, yielding a constraint of [31] (see also [32])

$$G\mu < 3 \times 10^{-7}, \qquad (1)$$

where μ is the string tension and G is Newton's constant. However, it is important to keep in mind that this limit is based on an analytical description of the scaling solution which contains a number of parameters which can only

be determined from comparisons with numerical simulations and whose values thus have a substantial uncertainty. Work based on a field theory simulation of strings [33] gives a limit of twice the above value (see also [34] for a very recent analysis of the different bounds). Note that limits on the cosmic string tension which come from gravitational radiation from string loops [35] are sensitive both to the large uncertainties in the distribution of string loops, and also to back-reaction effects on cosmic string loops (see e.g. [36]), and are hence not robust.

Direct limits on the cosmic string tension μ can be obtained by looking for specific signatures of individual long strings. These are limits which are insensitive to the parameters in the cosmic string scaling solution. Limits obtained from searching for the Kaiser-Stebbins signature of a long string in CMB temperature maps were derived in [37, 38] using WMAP data. The limits obtained were weaker than the ones from (1). However, the angular scale of the WMAP experiment is too large to be able to effectively search for sharp features in position space maps such as those predicted by cosmic strings. It was pointed out [39] that the string signatures for values of $G\mu$ somewhat smaller than the limiting value of (1) should be clearly visible in smaller angular scale CMB anisotropy maps such as those provided by the ACT [40] and SPT [41] experiments. In recent work [42–44] it was shown that limits up to an order of magnitude tighter than (1) might be achievable using SPT data. In the following, we will discuss direct signals of wakes created by long strings in 21cm surveys.

As first pointed out in [18] and then further discussed in [19–22], long strings moving perpendicular to the tangent vector along the string give rise to "wakes" behind the string, i.e. in the plane spanned by the tangent vector to the string and the velocity vector. The wake arises as a consequence of the geometry of space behind a long straight string [45, 46] - space perpendicular to the string is conical with a deficit angle given by

$$\alpha = 8\pi G\mu. \qquad (2)$$

From the point of view of an observer behind the string (relative to the string velocity vector), it appears that matter streaming by the string (from the point of view of the observer traveling with the string) obtains a velocity kick of magnitude

$$\delta v = 4\pi G\mu v_s \gamma_s \sim 4\text{km/s}(G\mu)_6 v_s \gamma_s \qquad (3)$$

towards the plane behind the string. In the above, v_s is the velocity of the string (in units of the speed of light), γ_s is the corresponding relativistic gamma factor, and $(G\mu)_6$ is the value of $G\mu$ in units of 10^{-6}. This leads to a wedge-shaped region behind the string with twice the background density (see Figure 1).

Since the strings are relativistic, they generally move with a velocity of the order of the speed of light. There will be frequent intersections of strings. The long strings will chop off loops, and this leads to the conclusion that
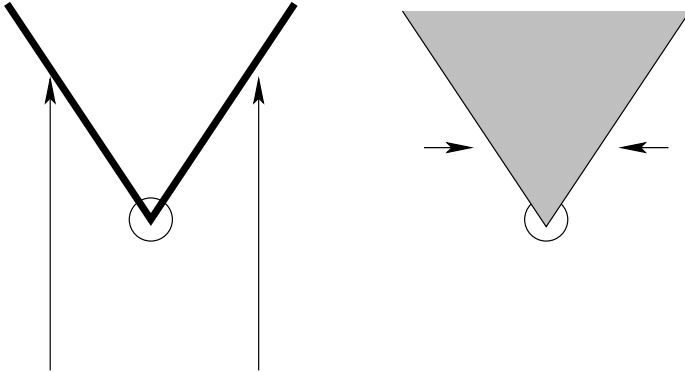
FIG. 1: Sketch of the mechanism by which a wake behind a moving string is generated. Consider a string perpendicular to the plane of the graph moving straight downward. From the point of view of the frame in which the string is at rest, matter is moving upwards, as indicated with the arrows in the left panel. From the point of view of an observer sitting behind the string (relative to the string motion) matter flowing past the string receives a velocity kick towards the plane determined by the direction of the string and the velocity vector (right panel). This velocity kick towards the plane leads to a wedge-shaped region behind the string with twice the background density (the shaded region in the right panel).

the string distribution will be statistically independent on time scales larger than the Hubble radius. Hence, to model the effects of strings we will make use of a toy model introduced in [47] and used in most analytical work on cosmic strings and structure formation since then: we divide the time interval between the time of equal matter and radiation and the current time t_0 into Hubble expansion time steps. In each time step, we lay down a distribution of straight string segments moving in randomly chosen directions with velocities chosen at random between 0 and 1 (in units of the speed of light). The centers and directions of these string segments are also chosen randomly, and the string density corresponds to N strings per Hubble volume, where N is an integer which is of the order 1 according to the scaling of the string network. The distribution of string segments is uncorrelated at different Hubble times. Each string segment will generate a wake, and it is the signal of one of these wakes which we will study in the following.

A string segment laid down at time t_i will generate a wake whose dimensions at that time are the following:

$$c_1 t_i \times t_i v_s \gamma_s \times 4\pi G \mu t_i v_s \gamma_s \,, \qquad (4)$$

where c_1 is a constant of order one. In the above, the first dimension is the length in direction of the string, the second is the depth. The fact that the string wake has a finite depth is due to the causality constraints on density fluctuations produced during a phase transition [48]: The information about the formation of a string (and hence the information about the existence of a deficit angle) cannot have propagated farther than the horizon from the point of nucleation of the defect. It was shown in

[49] that the deficit angle quite rapidly tends to zero as the horizon is approached.

The overdense region in the wake will lead to the gravitational accretion of matter above and below the wake towards the center of the wake. In this way, the wake will grow in thickness. The accretion of matter onto a cosmic string wake was studied in [21, 50] in the case of the dark matter being cold, and in [50, 51] in the case of the dark matter being hot. We are interested in the case of cold dark matter. As an aside, we mention that if the strings have lots of small-scale structure then they will have an effective tension which is less than the effective energy density [52]. This will lead to a local gravitational attraction of matter towards the string, a smaller transverse velocity, and hence to string filaments instead of wakes. The gravitational accretion onto string filaments was studied in [53].

We will now review the computation of the width of the wake. We are interested in the distribution of baryons in the vicinity of the string. However, for $t > t_{rec}$ the baryons and cold dark matter feel the same gravitational attraction and will thus behave in the same way - modulo thermal velocity effects which will be discussed later - until the baryons undergo a shock. Thus, for the moment we focus on the onset of clustering of the cold dark matter. We are interested in wakes created after the time t_{eq} of equal matter and radiation (there is no gravitational clustering of cold dark matter before that time). For times between t_{eq} and recombination (t_{rec}), the baryons are coupled to the radiation. However, for $t > t_{rec}$ the baryons will rapidly fall into the potential wells created by the cold dark matter and thus, once again, it is legitimate to focus attention on the clustering of the cold dark matter. Note that wakes produced at the earliest time are the most numerous.

We consider a mass shell located at a comoving distance q above the wake. Its physical distance above the wake at time t is

$$w(q,t) = a(t)\big(q - \psi\big) \,, \qquad (5)$$

where ψ is the co-moving perturbation induced by gravitational accretion. If the wake is laid down at the initial time t_i (with corresponding redshift z_i), then the initial conditions for the cold dark matter fluctuation are

$$\psi(t_i) = \dot{\psi}(t_i) = 0 \,. \qquad (6)$$

As a consequence of the initial wake planar overdensity $\sigma(t_i)$, the co-moving displacement ψ will begin to increase. The clustering dynamics can be studied making use of the Zel'dovich approximation [54] in which the gravitational force is treated in the Newtonian limit. As reviewed recently in [17], we obtain

$$\psi(t) = \frac{18\pi G}{5}\sigma(t_i)\Big(\frac{t_i}{t_0}\Big)^{2/3}\Big(\frac{t}{t_0}\Big)^{2/3}t_0^2 \,, \qquad (7)$$

where t_0 is the present time and $\sigma(t_i)$ is the initial wake planar density excess.

The mass shell with initial comoving distance q above the wake "turns around" when $\dot{w}(q,t) = 0$. At time t, this occurs for a value $q = q_{nl}(t)$ given by

$$q_{nl}(t) = \frac{24\pi}{5}G\mu v_s\gamma_s(z_i+1)^{-1/2}t_0\left(\frac{t}{t_i}\right)^{2/3}. \quad (8)$$

It is easy to check that at the point of turnaround

$$\psi(q_{nl},t) = \frac{1}{2}q, \quad (9)$$

and that hence the density inside the turnaround surface is twice the background density.

Once a matter shell reaches its maximal distance w_{max} from the center of the wake, it will start to collapse onto the wake. The infall of matter will halt as the shell hits other streams of matter. This will lead to a shock. In analogy with what can be shown analytically in the context of the spherical collapse model (see e.g. [55]) we assume that the shock occurs at approximately half the maximal distance. The hydrodynamical simulations of [56] confirm the applicability of this assumption. Since the distance at turnaround is half the width the shell would have without gravitational accretion onto the wake, the shock occurs at a distance $1/4$ of that which the matter shell would have under unperturbed Hubble expansion. Hence, the average density inside the wake is four times the background density, a result which will be used several times in the computations of the following section.

The evolution of the mass shell between turnaround and shock can be followed using (5) and (7). The shock will occur when $w(q,t) = (1/2)w_{max}(q)$. A straightforward computation shows that at this point the velocity is given by

$$\dot{w}(q,t) = -\frac{4\pi}{5}G\mu v_s\gamma_s\left(\frac{z_i+1}{z+1}\right)^{1/2}. \quad (10)$$

It is this velocity which then determines the temperature inside the shocked region.

The shocks will lead to thermalization of the wake. The gas temperature will be given by

$$\frac{3}{2}k_BT = \frac{1}{2}mv^2, \quad (11)$$

where m is the mass of a HI atom and v is the velocity of the in-falling particles when they hit the shock, which is given by

$$v = \dot{w}(q(t),t), \quad (12)$$

where $q(t)$ is the comoving distance of the shell which starts to collapse at the time t.

Inserting the result (10) into (12) and then into (11) we obtain the following result for the temperature T_K of the HI atoms inside the wake

$$T_K = \frac{16\pi^2}{75}(G\mu)^2(v_s\gamma_s)^2\frac{z_i+1}{z+1}k_B^{-1}m$$
$$\simeq [20\text{ K}](G\mu)_6^2(v_s\gamma_s)^2\frac{z_i+1}{z+1}, \quad (13)$$

where in the second line we have written the result in degrees K and expressed $G\mu$ in units of 10^{-6} (and kept only one significant figure in reporting the final number). The wake temperature is largest for wakes produced at the earliest times since the initial wake density is then the highest, and increases as time increases because more matter has time to accrete.

Assuming values of $G\mu = 3\times 10^{-7}$ (the current upper bound on the string tension), $z_i = 10^3$, (close to the time of recombination), $z+1 = 30$ and $(v_s\gamma_s)^2 = 1/3$, Eq. (13) yields $T_K \sim 20K$. This temperature is smaller than the CMB temperature $T_\gamma \simeq 82K$ at this redshift. As we will see in the following section, this leads to an absorption signal in the 21cm radiation.

The formation of a cosmic string wake and the thermalization which takes place inside the shocked region has been studied in [56] using an Eulerian hydro code [57] optimized to resolve shocks. The numerical simulations of [56] show that the density and temperature inside the shocked region are indeed roughly uniform and that the temperature obtained agrees with the values obtained here using analytical approximations.

Looking for signals from cosmic strings in 21cm surveys is potentially more powerful than looking in large-scale optical redshift surveys. This is because firstly the non-Gaussian signatures from strings are more pronounced at higher redshifts, secondly because we are directly looking at the distribution of the baryons, and not just the distribution of stars, the latter being affected by non-linear and gas dynamics, and thirdly because the distribution of matter is more linear at higher redshifts and hence easier to follow analytically. Compared to CMB and CMB polarization maps, 21cm surveys have the advantage of yielding three- rather than just two-dimensional maps, maps thus containing much more information. To our knowledge, there has been little previous work on 21cm emission from strings. Two exceptions are [58] in which the angular power spectrum of 21cm emission from a network of cosmic strings was considered, and [59], a recent study in which the correlation between 21cm emission and CMB signals from cosmic strings was studied. In contrast to these works, we are looking for direct string signals in position space 21cm maps.

In the following section we will briefly summarize some key features of 21cm cosmology and apply the equations for the 21cm brightness temperature to the case of emission from a string wake.

III.   COSMIC STRINGS AND 21CM MAPS

Neutral hydrogen is the dominant form of baryonic matter in the "dark ages", i.e. before star formation. Neutral hydogen has a 21cm hyperfine transition line which is excited if the hydrogen gas is at finite temperature. Hence, we expect redshifted 21cm radiation to reach us from all directions in the sky, and the intensity of this radiation can tell us about the distribution of

neutral hydrogen in the universe, as a function of both angular coordinates in the sky and redshift. Thus, in contrast to the CMB, 21cm surveys can probe the three-dimensional distribution of matter in the universe (see [60] for pioneering papers on the cosmology of the 21cm line and [15] for an in-depth review).

Let us now consider the equation of radiative transfer along the line of sight through a hydrogen gas cloud of uniform temperature- in the case of interest to us this gas cloud is the cosmic string wake. The brightness temperature $T_b(\nu)$ at an observed frequency ν due to 21cm emission is given by

$$T_b(\nu) = T_S\big(1 - e^{-\tau_\nu}\big) + T_\gamma(\nu)e^{-\tau_\nu}, \qquad (14)$$

where T_S is the spin temperature, T_γ is the microwave radiation temperature, and τ_ν is the optical depth obtained by integrating the absorption coefficient along the light ray through the gas cloud. The frequency ν is the blue-shifted frequency at the position of the cloud corresponding to the observed frequency ν_o. The term proportional to T_S is due to spontaneous emission, while the term proportional to T_γ is due to absorption and stimulated emission.

As explained in [15], what is of observational interest is the comparison of the temperature coming from the hydrogen cloud with the "clear view" of the 21 cm radiation from the CMB.

$$\delta T_b(\nu) = \frac{T_b(\nu) - T_\gamma(\nu)}{1 + z} \approx \frac{T_S - T_\gamma(\nu)}{1 + z}\tau_\nu. \qquad (15)$$

Note that the "clear view" of the CMB is hypothetical since even without a string wake's gas cloud the intergalactic medium is partly a less dense hydrogen gas. In the second part of the equation above we have expanded the exponential factor to linear order in the optical depth.

The spin temperature T_S is defined as the relative number density of atoms in the hyperfine energy states through $n_1/n_0 = 3\exp(-T_\star/T_S)$. Here n_1 and n_0 are the number densities of atoms in the two hyperfine states, and $T_\star = E_{10}/k_B = 0.068\text{K}$ is the temperature corresponding to the energy splitting E_{10} between these states.

The spin temperature is determined solely by the temperature T_K of the gas in the wake, as long as UV scattering is negligible (which is true in our case). The relationship between spin and kinetic gas temperatures is expressed through the collision coefficients x_c which describe the rate of scattering among hydrogen atoms and electrons:

$$T_S = \frac{1 + x_c}{1 + x_c T_\gamma/T_K}T_\gamma. \qquad (16)$$

We will shortly discuss the numerical values of the x_c for a particular case of interest.

Combining (15) and (16) we find for the difference $\delta T_b(\nu)$ in brightness temperature induced by the interaction of the radiation with neutral hydrogen is

$$\delta T_b(\nu) \simeq T_S\frac{x_c}{1 + x_c}\Big(1 - \frac{T_\gamma}{T_K}\Big)\tau_\nu(1 + z)^{-1}, \qquad (17)$$

where the last factor represents the red-shifting of the temperature between the time of emission and the present time. It is important to keep in mind that the brightness temperature from a region of space without density perturbations is nonzero. It is negative since the temperature of gas after redshift 200 is lower than that of the CMB photons, the former red-shifting as $(z(t) + 1)^2$, the latter as $z(t) + 1$. The optical depth of a cloud of hydrogen is

$$\tau_\nu = \frac{3c^2 A_{10}}{4\nu^2}\Big(\frac{\hbar\nu_{10}}{k_B T_S}\Big)\frac{N_{HI}}{4}\phi(\nu), \qquad (18)$$

where N_{HI} is the column density of HI.

Up to this point, the analysis has been general. Let us now specialize to the case where the gas cloud is the gas inside the cosmic string wake. In this case, the column density is the hydrogen number density n_{HI}^{wake} times the length that the light ray traversed in the cloud. This length will depend on the width w of the wake and the angle θ that the light ray makes relative to the vertical to the wake so that

$$N_{HI} = \frac{2n_{HI}^{wake}w}{\cos\theta}. \qquad (19)$$

The factor of 2 results since w is the width of the wake from the center.

The line profile $\phi(\nu)$ is due to broadening of the emission line. This broadening reflects the fact that not all photons resulting from the hyperfine transition will leave the gas cloud at the same frequency. Frequency differences are in general due to thermal motion, bulk motion and pressure effects. Since the pressures we are considering are small by astrophysical standards, pressure broadening is negligible. Since the gas temperature inside the wake is not much larger than the CMB temperature, thermal broadening will not be important, either. This leaves us with the effects of bulk motion, more specifically the expansion of the wake in planar directions. The line profile is normalized such that the integral of it over frequency is unity.

The origin of the line broadening due to the expansion of the wake is illustrated in Figure 2. Let us consider a point on the wake for which the photons travel to us at an angle which is not orthogonal to the plane of the wake. Then, relative to photons emitted at the central point on the photon path, photons emitted from the highest point and the lowest point obtain a relative Doppler shift of

$$\frac{\delta\nu}{\nu} = 2\sin(\theta)\tan\theta\frac{Hw}{c}, \qquad (20)$$

where H is the expansion rate of space and w is the wake width computed in the previous section, both evaluated at the redshift z when the photons are emitted. The angle θ is indicated in Figure 2. It is the angle relative to the vertical to the wake. As a consequence of the normalization of $\phi(\nu)$ we hence find

$$\phi(\nu) = \frac{1}{\delta\nu} \text{ for } \nu \,\epsilon\, \big[\nu_{10} - \frac{\delta\nu}{2}, \nu_{10} + \frac{\delta\nu}{2}\big], \qquad (21)$$
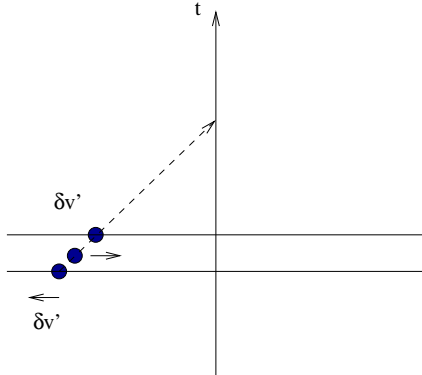
FIG. 2: Photons reaching us from a particular direction given by the angle θ to the vertical to the wake are emitted at different points in the wake. Three such points are indicated in the Figure - the central point and two points on the bottom and top of the wake, respectively. Since the wake is undergoing Hubble expansion in its planar directions, there is a relative Doppler frequency shift $\delta\nu$ between the 21cm photons from the top and the center of the wake.

and $\phi(\nu) = 0$ otherwise.

In addition to its role in determining the brightness temperature, the frequency shift $\delta\nu$ is important since it determines the width of the 21cm signal of strings in the redshift direction and is hence central to the issue of observability of the signal. From (20) and (8) (and setting the $2sin\theta tan\theta$ factor to one) we find that

$$\frac{\delta\nu}{\nu} = \frac{24\pi}{15}G\mu v_s\gamma_s\big(z_i+1\big)^{1/2}\big(z(t)+1\big)^{-1/2}$$
$$\simeq 3\times 10^{-5}(G\mu)_6(v_s\gamma_s)\,, \qquad (22)$$

where in the second line we have used the cosmological parameters mentioned at the end of the introductory section and inserted the representative redshifts $z_i+1 = 10^3$ and $z(t)+1 = 30$.

Taking the formula (17) for the brightness temperature, inserting the results (18) for the optical depth and (20) and (21) for the line profile, we get

$$\delta T_b(\nu) = 2\frac{x_c}{1+x_c}\big(1-\frac{T_\gamma}{T_K}\big)\frac{3c^3A_{10}\hbar}{16\nu_{10}^2k_BH_0\Omega_m^{1/2}}$$
$$\times n_{HI}^{bg}(t_0)\frac{n_{HI}^{wake}(t_0)}{n_{HI}^{bg}(t_0)}$$
$$\times(2\mathrm{sin}^2(\theta))^{-1}(1+z)^{1/2}\,, \qquad (23)$$

where Ω_m is the fraction of the critical energy density which is in the form of matter. Here the ratio of the density inside the wake to the background density, $n_{HI}^{wake}/n_{HI}^{bg}$, is approximately 4. We have rescaled the Hubble constant and the background HI density to its current values H_0 and $n_{HI}^{bg}(t_0)$, respectively, and made use of $H(z) = H_0\Omega_m^{1/2}(1+z)^{3/2}$ in the re-scaling. Note that the width of the wake has cancelled out between the HI column density and the line profile. The width of

the wake, however, has not disappeared completely from the calculation since it determines the wake temperature T_K, and since it yields the width of the signal in redshift direction.

Taking the values $A_{10} = 2.85\times 10^{-15}$ s^{-1}, $T_\star = 0.068$ K, $H_0 = 73$ km s^{-1} Mpc^{-1}, $\nu_{10} = 1420$ MHz, $\Omega_b = 0.042$, $\Omega_m = 0.26$, $2\sin^2\theta = 1$, eq. (23) becomes

$$\delta T_b(\nu) = [0.07 \text{ K}]\frac{x_c}{1+x_c}\big(1-\frac{T_\gamma}{T_K}\big)(1+z)^{1/2}\,. \qquad (24)$$

The collision coefficient x_c is dominated by the hydrogen-hydrogen collisions because of the very low fraction of free electrons. It is given by [61]

$$x_c = \frac{n\kappa_{10}^{HH}}{A_{10}}\frac{T_\star}{T_\gamma}\,. \qquad (25)$$

where κ_{10}^{HH} is the de-excitation cross section and is approximately 2.7×10^{-11}cm^{3}s^{-1} at a wake gas temperature of $T_K = 20K$ [61]. This temperature corresponds to the parameter values we took at the end of Section 2, i.e. $(G\mu)_6 = 0.3$, $(v_s\gamma_s)^2 = 1/3$, $z_i = 10^3$ and $z+1 = 30$. Remembering that the density n inside the wake is four times the background density $n_{bg} = 1.9\times 10^{-7}cm^{-3}(1+z)^3$ we find for a redshift $1+z = 30$ that $x_c \simeq 0.16$ and hence (from (24)) $\delta T_b(\nu) \simeq -160$ mK. For a formation redshift $z_i = z_{eq} = 3200$ corresponding to the time of equal matter and radiation the corresponding temperature is $\delta T_b(\mu) \simeq -15$ mK. Note that the dependence of the above result on the cosmic string tension μ enters only through the wake temperature. Note also that in the large $G\mu$ limit ($G\mu \gg 10^{-6}$), the brightness temperature approaches a constant value of close to 400mK.

There is a critical value of the string tension (which depends on the redshift) at which the cosmic string signal changes from emission to absorption. This value is determined by $T_K = T_\gamma$ which yields

$$(G\mu)_6^2 \simeq 0.1(v_s\gamma_s)^{-2}\frac{(z+1)^2}{z_i+1} \simeq 0.4\frac{(z+1)^2}{z_i+1}\,, \qquad (26)$$

for the value $(v_s\gamma_s)^2 = 1/3$ which we are using throughout, and this corresponds to $(G\mu)_6 \simeq 0.6$ if we use $(z_i+1) = 10^3$ and insert our reference redshift of $z+1 = 30$. At a redshift of $z+1 = 20$ the critical value is $(G\mu)_6 \simeq 0.4$. For a formation time corresponding to the redshift of equal matter and radiation the critical value of $G\mu$ is a factor of two lower.

For lower values of the tension the cosmic string signal in the 21cm maps shifts from an emission signal to an absorption signal. However, two effects must be taken into account when discussing the visibility of the string signal. The first is the fact that at very small values of $G\mu$ our calculation of the wake temperature breaks down. This occurs when the resulting wake temperature computed in (13) is smaller than the gas temperature obtained by taking the background gas temperature and computing its increase under adiabatic compression to

the overdensity of the wake. In this case it is no longer justified to take the initial conditions (6). At redshifts z below 150 the cosmic gas is cooling adiabatically as

$$T_g = 0.02\text{K}(1+z)^2 \tag{27}$$

because at this point Compton heating of the gas by the CMB is negligible [62]. Setting $T_K = 2.5 \times T_g$ (the factor 2.5 being due to the fact that for adiabatic compression of a mono-atomic gas by a factor of 4 in volume, one expects a temperature increase by a factor of $4^{2/3} \sim 2.5$) yields (for our standard values of $1 + z_i = 10^3$ and $(v_s\gamma_s)^2 = 1/3$)

$$(G\mu)_6 \simeq 3 \times 10^{-3}(1+z)^{3/2} \tag{28}$$

which equals $(G\mu)_6 = 0.5$ at a redshift of $1 + z = 30$. For a formation redshift $z_i = z_{eq}$ the factor 3 in (28) is replaced by 2.

For values of $G\mu$ smaller than the one given in (28), the effects of thermal pressure start to become important, and this will effect both the density and temperature structure in the wake.

Our results are illustrated in Figure 3 which shows a comparison of the temperatures relevant to the above discussion and their dependence on redshift. The vertical axis is the temperature axis, the horizontal axis is inverse redshift. The magenta (dashed) line shows the CMB temperature T_γ, the orange (dotted) line is the gas temperature in a wake $2.5T_g$ after adiabatic contraction. The two solid lines with the positive slope represent T_K for two different values of $G\mu$. The upper curve is for $(G\mu)_6 = 1$, the lower curve for $(G\mu)_6 = 0.3$. Along a fixed $G\mu$ curve, the 21cm signal of a cosmic string is an emission signal above the T_γ curve and an absorption signal below it. Above the $2.5T_g$ curve, the temperature of the gas inside the wake is well approximated by the equation (13), below it the initial thermal gas temperature effects dominate and the wake temperature will follow the $2.5T_g$ curve. The wake temperature curves are for a formation redshift of $z_i + 1 = 10^3$.

The second issue is that the string signal must be compared to what would be seen if the wake region were replaced by unclustered neutral gas. In this case, the absorption signal has a temperature given by (24) with T_K replaced by T_g and the collision coefficient computed with T_g instead of T_K. Due to the overdensity of the wake, the signal of a string wake should persist. The overdensity in the string wake by a factor of 4 will lead to an enhancement in the magnitude of the brightness temperature by a factor of 16 compared to what would be seen if the wake region were replaced by unclustered gas. One factor of 4 comes from the fact that the collision coefficient is proportional to the gas density, the second from the fact that the optical depth is also proportional to the density. In addition, the temperature ratios in (24) are different.

However, for values of $G\mu$ so small that $T_K \ll T_g$ there will no longer be any shock and hence no well-defined
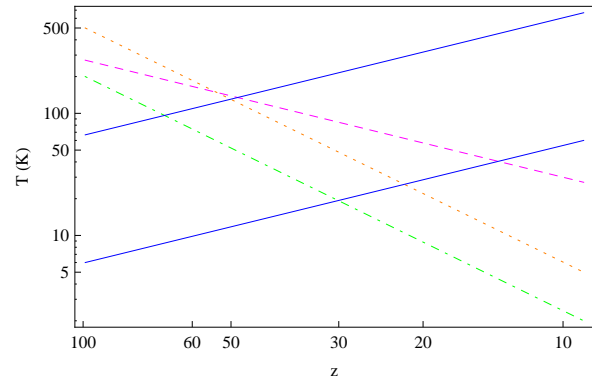

FIG. 3: The redshift dependence of the relevant temperatures. The majenta dashed line is the CMB temperature T_γ, the orange dotted line is $2.5T_g$, the gas temperature after adiabatic contraction by a factor 4 in volume, and the green (dot-dashed) line is the T_g curve. The two solid curves with positive slope represent T_K for two different values of $G\mu$, $(G\mu)_6 = 1$ in the case of the upper curve and $(G\mu)_6 = 0.3$ in the case of the lower curve (in both cases for a formation redshift $z_i + 1 = 10^3$). Following one of the solid curves, we see that the 21cm string signal is an emission signal above the majenta curve and an absorption signal below it. The wake temperature is given by T_K only above the orange curve. For higher redshifts, the initial gas temperature dominates the final temperature of the gas inside the wake, and the latter follows the orange curve. Once T_K drops below the green curve, there will no longer be any shock and our effect disappears.

wake region with overdensity 4. This will occur at a value of $G\mu$ which is smaller than the limit in (28) by a factor of $\sqrt{2.5}$. Note also that the thickness in redshift space (discussed below) of the signal decreases as $G\mu$ decreases, and hence improved sensitivity will be required to detect the signal.

The bottom line of the above analysis is that at a redshift of $z+1 = 30$, strings with tensions below the current observational limit are predicted to be visible in absorption in 21cm surveys. Strings with larger tensions would yield an emission signal. The critical value (26) of $G\mu$ at which the emission signal turns into an absorption signal decreases as z decreases, so that strings with tensions at the current observational limit would become visible in emission at a redshift of below 20. However, the value of z cannot be smaller than that corresponding to reionization since we have not considered how UV scattering affects the spin temperature.

The 21cm signature of a cosmic string wake has a distinctive shape in redshift space. The string signal will be a wedge-like region of extra 21cm emission. The signal will be wide in the two angular directions, and narrow in redshift direction [1]. The projection of this region onto

---

[1] The signal at a fixed redshift would be extended only in one angular direction.

the plane corresponding to the two angles in the sky (we are working in the limit of small angles and thus can use the flat sky approximation) corresponds to the projection of the wake onto the observer's past light cone. The orientation of the wedge in redshift space is given by the orientation of the wake relative to the observer's light cone. This is illustrated in Figure 4. The left panel is a space-time sketch of the geometry (with two spatial directions suppressed). The wake is created by a string segment which starts out at time t_i at the position x_1 and which at time $2t_i$ (roughly one Hubble time step later) has moved to the position x_2 (the arrow on the segment connecting the two events gives the direction of the velocity of the string segment. For the orientation of the string chosen, the past light cone intersects the "back" of the string wake at a later time than the front. Hence, the 21cm signal has a larger red-shift for photons from the tip of the wake than from the back side of the wake. The width of the wake vanishes at the tip and increases towards the back. Hence, in redshift space the region of extra 21cm emission has the orientation sketched on the right panel of Figure 4. The planar dimensions of the region of extra emission are in the angular directions, and their sizes are the angles corresponding to the comoving area (see (4))

$$c_1 t_i(z_i + 1) \times t_i v_s \gamma_s(z_i + 1). \tag{29}$$

The amplitude of the emission signal depends on the orientation of the wake relative to us (through the redshift when our past light cone intersects the various parts of the wake). This is not correlated with the direction of string motion. The width in redshift space, on the other hand, depends on the emission point on the wake - the width is larger in the back and approaches zero at the tip, as given by $\delta\nu$ (see 20).

IV. CONCLUSIONS AND DISCUSSION

In this paper we have calculated the 21cm signal of a single cosmic string wake. We found that wakes leave a characteristic signal in 21cm surveys - wedge shaped regions of extra emission or absorption, depending on the value of the string tension. There is an emission signal as long as the string tension exceeds the critical value given by (26) and as the tension increases the temperature approaches the value given by 200mK, a value larger by almost two orders of magnitude compared to the backgrounds from standard cosmology sources which the Square Kilometer Array (SKA) telescope project is designed to be sensitive to [63]. For values of $G\mu$ below the critical value given by (26), the cosmic string wake signal changes to an absorption signal. This will persist down to a value of $G\mu$ a factor of $\sqrt{2.5}$ smaller than the value given in (28), at which point the material which is gravitationally attracted to the wake will no longer undergo a shock and hence our analysis ceases to be applicable. The width of the wedge in redshift space depends
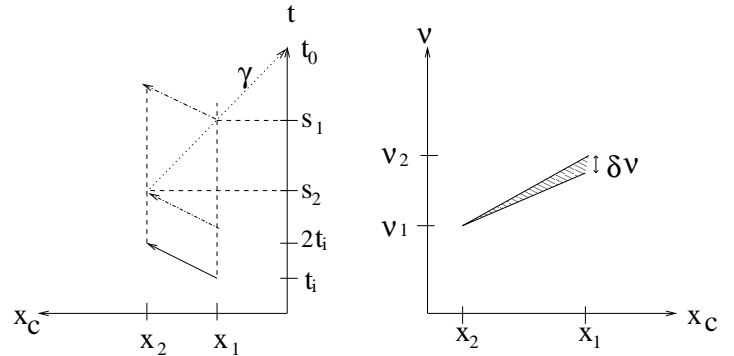

FIG. 4: Geometry of the 21cm signal of a cosmic string wake. The left panel is a sketch of the geometry of the wake in space-time - vertical axis denoting time, the horizontal axis one direction of space. The string segment producing the wake is born at time t_i and travels in the direction of the arrow, ending at the position x_2 at the time $2t_i$. The past light cone of the observer at the time t_0 intersects the tip of the wake at the time s_2, the back of the wake at time s_1. These times are in general different. Hence, the 21cm radiation from different parts of the wake is observed at different red-shifts. The resulting angle-redshift signal of the string wake shown in the left panel is illustrated in the right panel, where the horizontal axis is the same spatial coordinate as in the left panel, but the vertical axis is the redshift of the 21cm radiation signal. The wedge in 21cm has vanishing thickness at the tip of the wedge, and thickness given by $\delta\nu$ at the back side.

on the string tension via (20). The width increases from zero at the tip of the string to the value given by (20) at the midpoint of the wake.

The sensitivity of 21cm surveys to cosmic strings is best at the lowest redshifts sufficiently higher than the redshift of reionization. This is due to the fact that the string wakes keep increasing in width as a function of time, leading to an increasing temperature of the gas in the wake and hence to a higher 21cm signal. At the same time, the wakes become more stable towards thermal disruption.

As mentioned above, the brightness temperature shift which we predict will be large compared to that from the surrounding intergalactic medium. The fractional frequency width of the signal is given by (22) and is near the limit of the frequency resolution of radio telescopes for values of $G\mu$ close to the current upper bound. For example, the Square Kilometer Array will have a fractional spectral resolution of the order [63] of 10^{-4}. In both angular directions, the signal will cover a rectangle whose side length is given by the comoving Hubble radius at the redshift z_i, which for redshifts close to recombination corresponds to a scale of about one degree. Thus, the signal of cosmic strings which we predict is clearly a possible target for future radio telescopes. For example, the angular resolution of the SKA is designed to be smaller than 0.1 arcsec, and the frequency range of the SKA will allow the detection of the 21cm signal up to a

redshift of 20.

We have focused on the signal of a single wake laid down at a time $t > t_{eq}$. The reader may worry that the signal of such a wake is masked by the "noise" due to wakes laid down at earlier times. Even though the baryons will stream out of these wakes due to their coupling with the photons, the dark matter wakes persist. For $t < t_{eq}$ the dark matter wakes do not grow in thickness until $t = t_{eq}$. After that, the thickness will begin to grow, and at $t > t_{rec}$ the baryons will start to fall into the dark matter potential wells. However, the width of such wakes (averaged over the length of the wake) is smaller than that of wakes at $t = t_{eq}$. In addition, due to their large number, on length scales of wakes laid down at $t \geq t_{eq}$, the earlier wakes will act like Gaussian noise. The coherent signature in position space of such a "late" wake can be picked out of the Gaussian noise even if the amplitude of the Gaussian noise is comparable to or slightly larger than the amplitude of the signal (as measured in terms of the contribution to the power spectrum). This has been studied in the context of picking out the signatures of late strings in CMB temperature maps in [42–44], and we expect similar conclusions to hold here.

Let us end with a brief comparison of our work with that of [58] and [59] who also considered 21cm signals of cosmic strings. What sets our work apart is that we focus on the specific position space signature of wakes rather than on the (Fourier space) power spectrum. In computing a power spectrum, one loses the information about the non-Gaussianities in the distribution of strings. It is these non-Gaussianities which most clearly distinguish the predictions of a string model from a model with only Gaussian fluctuations. Therefore, the sensitivity to the presence of cosmic strings will be much higher in a study like ours compared to what can be achieved by only computing power spectra.

[1] Y. B. Zeldovich, "Cosmological fluctuations produced near a singularity," Mon. Not. Roy. Astron. Soc. **192**, 663 (1980).

[2] A. Vilenkin, "Cosmological Density Fluctuations Produced By Vacuum Strings," Phys. Rev. Lett. **46**, 1169 (1981) [Erratum-ibid. **46**, 1496 (1981)].

[3] T. W. B. Kibble, "Phase Transitions In The Early Universe," Acta Phys. Polon. B **13**, 723 (1982); T. W. B. Kibble, "Some Implications Of A Cosmological Phase Transition," Phys. Rept. **67**, 183 (1980).

[4] N. Turok and R. H. Brandenberger, "Cosmic Strings And The Formation Of Galaxies And Clusters Of Galaxies," Phys. Rev. D **33**, 2175 (1986).

[5] H. Sato, "Galaxy Formation by Cosmic Strings," Prog. Theor. Phys. **75**, 1342 (1986).

[6] A. Stebbins, "Cosmic Strings and Cold Matter", Ap. J. (Lett.) **303**, L21 (1986).

[7] J. Magueijo, A. Albrecht, D. Coulson and P. Ferreira, "Doppler peaks from active perturbations," Phys. Rev. Lett. **76**, 2617 (1996) [arXiv:astro-ph/9511042].

[8] U. L. Pen, U. Seljak and N. Turok, "Power spectra in global defect theories of cosmic structure formation," Phys. Rev. Lett. **79**, 1611 (1997) [arXiv:astro-ph/9704165].

[9] R. Jeannerot, "A Supersymmetric SO(10) Model with Inflation and Cosmic Strings," Phys. Rev. D **53**, 5426 (1996) [arXiv:hep-ph/9509365]; R. Jeannerot, J. Rocher and M. Sakellariadou, "How generic is cosmic string formation in SUSY GUTs," Phys. Rev. D **68**, 103514 (2003) [arXiv:hep-ph/0308134].

[10] E. Witten, "Cosmic Superstrings," Phys. Lett. B **153**, 243 (1985).

[11] S. Sarangi and S. H. H. Tye, "Cosmic string production towards the end of brane inflation," Phys. Lett. B **536**, 185 (2002) [arXiv:hep-th/0204074].

[12] E. J. Copeland, R. C. Myers and J. Polchinski, "Cosmic F- and D-strings," JHEP **0406**, 013 (2004) [arXiv:hep-th/0312067].

[13] A. C. Davis and T. W. B. Kibble, "Fundamental cosmic strings," Contemp. Phys. **46**, 313 (2005) [arXiv:hep-th/0505050]; M. Sakellariadou, "Cosmic Superstrings," arXiv:0802.3379 [hep-th].

[14] R. H. Brandenberger and C. Vafa, "Superstrings In The Early Universe," Nucl. Phys. B **316**, 391 (1989).; A. Nayeri, R. H. Brandenberger and C. Vafa, "Producing a scale-invariant spectrum of perturbations in a Hagedorn phase of string cosmology," Phys. Rev. Lett. **97**, 021302 (2006) [arXiv:hep-th/0511140]; R. H. Brandenberger, A. Nayeri, S. P. Patil and C. Vafa, "String gas cosmology and structure formation," arXiv:hep-th/0608121; R. H. Brandenberger, "String Gas Cosmology," arXiv:0808.0746 [hep-th].

[15] S. Furlanetto, S. P. Oh and F. Briggs, "Cosmology at Low Frequencies: The 21 cm Transition and the High-Redshift Universe," Phys. Rept. **433**, 181 (2006) [arXiv:astro-ph/0608032].

[16] N. Kaiser and A. Stebbins, "Microwave Anisotropy Due To Cosmic Strings," Nature **310**, 391 (1984).

[17] R. J. Danos, R. H. Brandenberger and G. Holder, "A Signature of Cosmic Strings Wakes in the CMB Polarization," arXiv:1003.0905 [astro-ph.CO].

[18] J. Silk and A. Vilenkin, "Cosmic Strings And Galaxy Formation," Phys. Rev. Lett. **53**, 1700 (1984).

[19] M. Rees, "Baryon concentrations in string wakes at $z \geq$

200: implications for galaxy formation and large-scale structure," Mon. Not. R. astr. Soc. **222**, 27p (1986).

[20] T. Vachaspati, "Cosmic Strings and the Large-Scale Structure of the Universe," Phys. Rev. Lett. **57**, 1655 (1986).

[21] A. Stebbins, S. Veeraraghavan, R. H. Brandenberger, J. Silk and N. Turok, "Cosmic String Wakes," Astrophys. J. **322**, 1 (1987).

[22] J. C. Charlton, "Cosmic String Wakes and Large Scale Structure," Astrophys. J. **325**, 52 (1988).

[23] T. Hara and S. Miyoshi, "Formation of the First Systems in the Wakes of Moving Cosmic Strings," Prog. Theor. Phys. **77**, 1152 (1987);
T. Hara and S. Miyoshi, "Flareup of the Universe After Z Appproximately 10**2 for Cosmic String Model," Prog. Theor. Phys. **78**, 1081 (1987);
T. Hara and S. Miyoshi, "Large Scale Structures and Streaming Velocities Due to Open Cosmic Strings," Prog. Theor. Phys. **81**, 1187 (1989).

[24] D. N. Spergel *et al.* [WMAP Collaboration], "Wilkinson Microwave Anisotropy Probe (WMAP) three year results: Implications for cosmology," Astrophys. J. Suppl. **170**, 377 (2007) [arXiv:astro-ph/0603449].

[25] T. W. B. Kibble, "Phase Transitions In The Early Universe," Acta Phys. Polon. B **13**, 723 (1982);
T. W. B. Kibble, "Topology Of Cosmic Domains And Strings," J. Phys. A **9**, 1387 (1976).

[26] A. Vilenkin and E.P.S. Shellard, *Cosmic Strings and other Topological Defects* (Cambridge Univ. Press, Cambridge, 1994).

[27] M. B. Hindmarsh and T. W. B. Kibble, "Cosmic strings," Rept. Prog. Phys. **58**, 477 (1995) [arXiv:hep-ph/9411342].

[28] R. H. Brandenberger, "Topological defects and structure formation," Int. J. Mod. Phys. A **9**, 2117 (1994) [arXiv:astro-ph/9310041].

[29] A. Albrecht and N. Turok, "Evolution Of Cosmic Strings," Phys. Rev. Lett. **54**, 1868 (1985);
D. P. Bennett and F. R. Bouchet, "Evidence For A Scaling Solution In Cosmic String Evolution," Phys. Rev. Lett. **60**, 257 (1988);
B. Allen and E. P. S. Shellard, "Cosmic String Evolution: A Numerical Simulation," Phys. Rev. Lett. **64**, 119 (1990);
C. Ringeval, M. Sakellariadou and F. Bouchet, "Cosmological evolution of cosmic string loops," JCAP **0702**, 023 (2007) [arXiv:astro-ph/0511646];
V. Vanchurin, K. D. Olum and A. Vilenkin, "Scaling of cosmic string loops," Phys. Rev. D **74**, 063527 (2006) [arXiv:gr-qc/0511159].

[30] J. Polchinski and J. V. Rocha, "Analytic Study of Small Scale Structure on Cosmic Strings," Phys. Rev. D **74**, 083504 (2006) [arXiv:hep-ph/0606205].

[31] L. Pogosian, S. H. H. Tye, I. Wasserman and M. Wyman, "Observational constraints on cosmic string production during brane inflation," Phys. Rev. D **68**, 023506 (2003) [Erratum-ibid. D **73**, 089904 (2006)] [arXiv:hep-th/0304188];
M. Wyman, L. Pogosian and I. Wasserman, "Bounds on cosmic strings from WMAP and SDSS," Phys. Rev. D **72**, 023513 (2005) [Erratum-ibid. D **73**, 089905 (2006)] [arXiv:astro-ph/0503364].

[32] A. A. Fraisse, "Limits on Defects Formation and Hybrid Inflationary Models with Three-Year WMAP Observations," JCAP **0703**, 008 (2007) [arXiv:astro-ph/0603589];
U. Seljak, A. Slosar and P. McDonald, "Cosmological parameters from combining the Lyman-alpha forest with CMB, galaxy clustering and SN constraints," JCAP **0610**, 014 (2006) [arXiv:astro-ph/0604335];
R. A. Battye, B. Garbrecht and A. Moss, "Constraints on supersymmetric models of hybrid inflation," JCAP **0609**, 007 (2006) [arXiv:astro-ph/0607339];
R. A. Battye, B. Garbrecht, A. Moss and H. Stoica, "Constraints on Brane Inflation and Cosmic Strings," JCAP **0801**, 020 (2008) [arXiv:0710.1541 [astro-ph]].

[33] N. Bevis, M. Hindmarsh, M. Kunz and J. Urrestilla, "CMB power spectrum contribution from cosmic strings using field-evolution simulations of the Abelian Higgs model," Phys. Rev. D **75**, 065015 (2007) [arXiv:astro-ph/0605018];
N. Bevis, M. Hindmarsh, M. Kunz and J. Urrestilla, "Fitting CMB data with cosmic strings and inflation," arXiv:astro-ph/0702223.

[34] R. Battye and A. Moss, "Updated constraints on the cosmic string tension," arXiv:1005.0479 [astro-ph.CO].

[35] T. Damour and A. Vilenkin, "Gravitational wave bursts from cosmic strings," Phys. Rev. Lett. **85**, 3761 (2000) [arXiv:gr-qc/0004075];
T. Damour and A. Vilenkin, "Gravitational wave bursts from cusps and kinks on cosmic strings," Phys. Rev. D **64**, 064008 (2001) [arXiv:gr-qc/0104026].

[36] R. H. Brandenberger, "On the Decay of Cosmic String Loops," Nucl. Phys. B **293**, 812 (1987).

[37] A. S. Lo and E. L. Wright, "Signatures of cosmic strings in the cosmic microwave background," arXiv:astro-ph/0503120.

[38] E. Jeong and G. F. Smoot, "Search for cosmic strings in CMB anisotropies," Astrophys. J. **624**, 21 (2005) [arXiv:astro-ph/0406432];
E. Jeong and G. F. Smoot, "The Validity of the Cosmic String Pattern Search with the Cosmic Microwave Background," arXiv:astro-ph/0612706.

[39] A. A. Fraisse, C. Ringeval, D. N. Spergel and F. R. Bouchet, "Small-Angle CMB Temperature Anisotropies Induced by Cosmic Strings," arXiv:0708.1162 [astro-ph].

[40] A. Kosowsky [the ACT Collaboration], "The Atacama Cosmology Telescope Project: A Progress Report," New Astron. Rev. **50**, 969 (2006) [arXiv:astro-ph/0608549].

[41] J. E. Ruhl *et al.* [The SPT Collaboration], "The South Pole Telescope," Proc. SPIE Int. Soc. Opt. Eng. **5498**, 11 (2004) [arXiv:astro-ph/0411122].

[42] S. Amsel, J. Berger and R. H. Brandenberger, "Detecting Cosmic Strings in the CMB with the Canny Algorithm," JCAP **0804**, 015 (2008) [arXiv:0709.0982 [astro-ph]].

[43] A. Stewart and R. Brandenberger, "Edge Detection, Cosmic Strings and the South Pole Telescope," arXiv:0809.0865 [astro-ph].

[44] R. J. Danos and R. H. Brandenberger, "Canny Algorithm, Cosmic Strings and the Cosmic Microwave Background," arXiv:0811.2004 [astro-ph];
R. J. Danos and R. H. Brandenberger, "Searching for Signatures of Cosmic Superstrings in the CMB," arXiv:0910.5722 [astro-ph.CO].

[45] A. Vilenkin, "Gravitational Field Of Vacuum Domain Walls And Strings," Phys. Rev. D **23**, 852 (1981).

[46] R. Gregory, "Gravitational Stability of Local Strings,"

Phys. Rev. Lett. **59**, 740 (1987).

[47] L. Perivolaropoulos, "COBE versus cosmic strings: An Analytical model," Phys. Lett. B **298**, 305 (1993) [arXiv:hep-ph/9208247];
L. Perivolaropoulos, "Statistics of microwave fluctuations induced by topological defects," Phys. Rev. D **48**, 1530 (1993) [arXiv:hep-ph/9212228].

[48] J. H. Traschen, "Causal Cosmological Perturbations And Implications For The Sachs-Wolfe Effect," Phys. Rev. D **29**, 1563 (1984);
J. H. Traschen, "Constraints On Stress Energy Perturbations In General Relativity," Phys. Rev. D **31**, 283 (1985).

[49] J. C. R. Magueijo, "Inborn metric of cosmic strings," Phys. Rev. D **46**, 1368 (1992).

[50] R. H. Brandenberger, L. Perivolaropoulos and A. Stebbins, "Cosmic Strings, Hot Dark Matter and the Large-Scale Structure of the Universe," Int. J. Mod. Phys. A **5**, 1633 (1990).

[51] L. Perivolaropoulos, R. H. Brandenberger and A. Stebbins, "Dissipationless Clustering Of Neutrinos In Cosmic String Induced Wakes," Phys. Rev. D **41**, 1764 (1990).

[52] B. Carter, "Integrable equation of state for noisy cosmic string," Phys. Rev. D **41**, 3869 (1990);
A. Vilenkin, "Effect of Small Scale Structure on the Dynamics of Cosmic Strings," Phys. Rev. D **41**, 3038 (1990).

[53] A. N. Aguirre and R. H. Brandenberger, "Accretion of hot dark matter onto slowly moving cosmic strings," Int. J. Mod. Phys. D **4**, 711 (1995) [arXiv:astro-ph/9505031].

[54] Y. B. Zeldovich, "Gravitational instability: An Approximate theory for large density perturbations," Astron. Astrophys. **5**, 84 (1970).

[55] P.J.E. Peebles, "The Large-Scale Structure of the Universe" (Princeton Univ. Press, Princeton, 1980).

[56] A. Sornborger, R. H. Brandenberger, B. Fryxell and K. Olson, "The structure of cosmic string wakes," Astrophys. J. **482**, 22 (1997) [arXiv:astro-ph/9608020].

[57] A. Sornborger, B. Fryxell, K. Olson and P. MacNeice, "An Eulerian PPM & PIC Code for Cosmological Hydrodynamics," arXiv:astro-ph/9608019.

[58] R. Khatri and B. D. Wandelt, "Cosmic (super)string constraints from 21 cm radiation," Phys. Rev. Lett. **100**, 091302 (2008) [arXiv:0801.4406 [astro-ph]].

[59] A. Berndsen, L. Pogosian and M. Wyman, "Correlations between 21 cm Radiation and the CMB from Active Sources," arXiv:1003.2214 [astro-ph.CO].

[60] C. Hogan and M. Rees, Mon. Not. R. Astron. Soc. **188**, 791 (1979);
D. Scott and M. Rees, "The 21-cm line at high redshift: a diagnostic for the origin of large-scale structure", Mon. Not. R. Astron. Soc. **247**, 510 (1990);
P. Madau, A. Meiksin and M. Rees, "21-cm Tomography of the Intergalactic Medium at High Redshift," Astrophys. J. **475**, 429 (1997) [arXiv:astro-ph/9608010].

[61] B. Zygelman, "Hyperfine Level-changing Collisions of Hydrogen Atoms and Tomography of the Dark Age Universe", Astrophys. J. **622**, 1356 (2005);
S. Furlanetto and M. Furlanetto, "Spin Exchange Rates in Electron-Hydrogen Collisions," Mon. Not. Roy. Astron. Soc. **374**, 547 (2007) [arXiv:astro-ph/0608067].

[62] S. Seager, D. D. Sasselov and D. Scott, "A New Calculation of the Recombination Epoch," Astrophys. J. **523**, L1 (1999) [arXiv:astro-ph/9909275];
S. Seager, D. D. Sasselov and D. Scott, "How exactly did the Universe become neutral?," Astrophys. J. Suppl. **128**, 407 (2000) [arXiv:astro-ph/9912182].

[63] C. L. Carilli and S. Rawlings, "Science with the Square Kilometer Array - Editorial", New Astronomy Reviews **48**, 979 (2004);
C. L. Carilli et al, "Probing the Dark Ages with the Square Kilometer Array", New Astronomy Reviews **48**, 1029 (2004).